Mon. Not. R. astr. Soc. (1977) **178**, 451–466

The remarkable Seyfert galaxy Markarian 231

A. Boksenberg and R. F. Carswell *Department of Physics and Astronomy, University College London*

D. A. Allen, R. A. E. Fosbury and M. V. Penston
Royal Greenwich Observatory, Herstmonceux Castle, Hailsham, Sussex BN27 1RP and Anglo-Australian Observatory, PO Box 29, Epping, New South Wales 2121, Australia

W. L. W. Sargent *Hale Observatories, California Institute of Technology, Carnegie Institution of Washington, Pasadena, California 91109, USA*

Received 1976 June 7

Summary. Spectra, scans and a direct electronograph of Markarian 231 are presented. The continuum can be represented by a $f_\nu \propto \nu^{-2.5}$ power law but the presence of optical and infrared absorption features favours interpretation as either a reddened $f_\nu \sim$ constant spectrum or a reddened 10 000 K blackbody distribution from hot stars. Either of these models has intrinsic absolute magnitude, $M_v \sim -25.1$, placing Markarian 231 among the quasars in optical luminosity. The observed emission spectrum can be synthesized from blended features of H I, He I, [O II], Ca II, Fe II, [Fe II] and Ni II at a redshift of 12 600 ± 200 km/s. Except for the [O II], which must be emitted from a separate low-density region, these lines indicate a high-density ($n_e \sim 10^7 \text{cm}^{-3}$) emission region. The presence of Ca II triplet emission and no corresponding *H* and *K* emission shows that the optical depths in *H* and *K* in the emission region are large ($\tau_H \sim 100$). There are three absorption line redshifts – System I containing resonance lines of Ca II and Na I and λ 3889 of He I at a redshift of ~ 8000 km/s, System II represented by *D*-lines and λ 3889 at 6250 km/s and System III featuring the *K*-line and members of the Balmer series at 12 900 km/s. If the observed continuum is emitted by hot stars the System III lines represent the absorption spectra of those stars. The lines are much broader than the absorption lines seen in high-redshift quasars. The doublet ratio for *H* and *K* in System I indicates a low optical depth $\tau_H \sim 0.6$ along our line of sight to the nucleus in contrast to the result from the emission lines. The calcium and iron emission lines can be produced by fluorescence if the ions experience the unreddened radiation of the continuum source. Two possible configurations for the nuclear components of Markarian 231 are presented.

1 Introduction

Most Seyfert galaxies fall into two classes defined by Khachikian & Weedman (1973). In the class 1 objects the Balmer lines are very broad (~10 000 km/s wide) and the forbidden lines relatively narrow: in class 2 Seyferts both the Balmer and forbidden lines are broad (~1000 km/s). Other broad lines, in particular those of He I, He II and Fe II, are often seen in the spectra of class 1 Seyferts (e.g. Boksenberg *et al.* 1975b). Spectrophotometry of a large number of Seyfert galaxies (Sargent, unpublished) shows that there is a gradation of the strength of the broad Fe II emission features among class 1 Seyferts from objects in which they are invisible to those in which they dominate the spectrum and the forbidden lines are weak or absent. Well-known examples of the latter type are I Zw 0051+12 and II Zw 2130+09 (Sargent 1968, 1970) and the spectra of these objects superficially resemble that of the quasar 3C 273 (Baldwin 1975a; Boksenberg *et al.* 1975a). Since the broad-line spectrum appears to come from a dense ($n_e \gtrsim 10^7 \text{cm}^{-3}$) region close to the non-thermal continuum source in the Seyfert nucleus, it was decided to study a member of the class of Fe II emission objects in some detail to see if the physical conditions in, and geometry of, this region could be determined.

The object chosen, Markarian 231, had previously been studied spectroscopically by Adams & Weedman (1972) and by Adams (1972). They had found extremely strong Fe II emission with the Balmer series and λ 3727 of [O II] also present at a redshift of 12 300 km/s. In addition they showed that Markarian 231 has a strong absorption line spectrum featuring the *H*, *K* and *D*-lines and λ 3889 of He I at a redshift of 7900 km/s and a second system showing Balmer line absorption at 12 500 km/s. Other peculiar features of Markarian 231 include unusually red *UBV* colours for a Seyfert nucleus (Weedman 1973), a strong infrared excess (e.g. Rieke & Low 1972) and a silicate absorption at 10 μm (Allen 1976, and references therein).

2 Observational data

The optical appearance of Markarian 231 is illustrated in Fig. 1 – this is from a PDS microdensitometer scan of an unfiltered direct electronograph. It was obtained using the RGO 4-cm S20 electronographic camera (McMullan, Powell & Curtis 1972) mounted at the Cassegrain focus of the 40-in telescope of the Wise Observatory, Israel. It shows Markarian 231 to be a galaxy with a bright nucleus and a single spiral arm running clockwise from the south-west. There is a shield-like structure on the western side of the galaxy, resembling features in interacting galaxies, whose south-west end leads to a non-stellar condensation whose nature is at present unknown. Visual observations at the telescope show that the nucleus is unresolved.

Scans were obtained on the Multi-Channel Spectrophotometer (MCSP) (Oke 1969) at the Cassegrain focus of the 200-in Hale telescope on Palomar Mountain. One scan was taken on 1974 April 21/22 with a resolution of 20 Å in the blue (λλ 3150–5710) and 40 Å in the red (λλ 5660–11020), the other on 1975 June 3/9 with a resolution of 20 Å throughout the observed range. They were reduced to fluxes based on the absolute calibration of α Lyrae by Oke & Schild (1970). The scans used 10-arcsec diameter circular apertures with a sky aperture 40 arcsec away in right ascension. The lower resolution scan is illustrated in Fig. 2.

Spectra of the nucleus of Markarian 231 were also obtained on the 98-in Isaac Newton telescope at Herstmonceux during 1975 February, April and June using the University College London, Image Photon Counting System (IPCS) mounted at the camera focus of the Unit Spectrograph. Different gratings were used giving a range of resolutions between

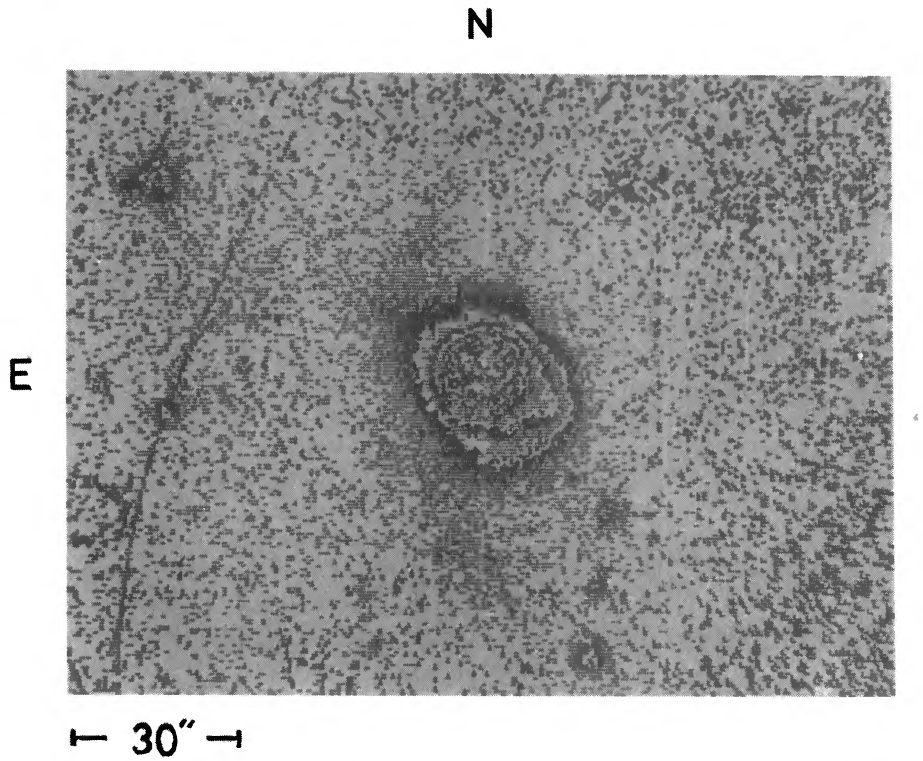

Figure 1. Direct electronograph of Markarian 231 in unfiltered light using an S20 tube. The three grey levels are spaced by 0.05 in optical density on Ilford L4 emulsion and repeat in the sequence white, grey, black. The thin line to the east of the picture is an emulsion defect.

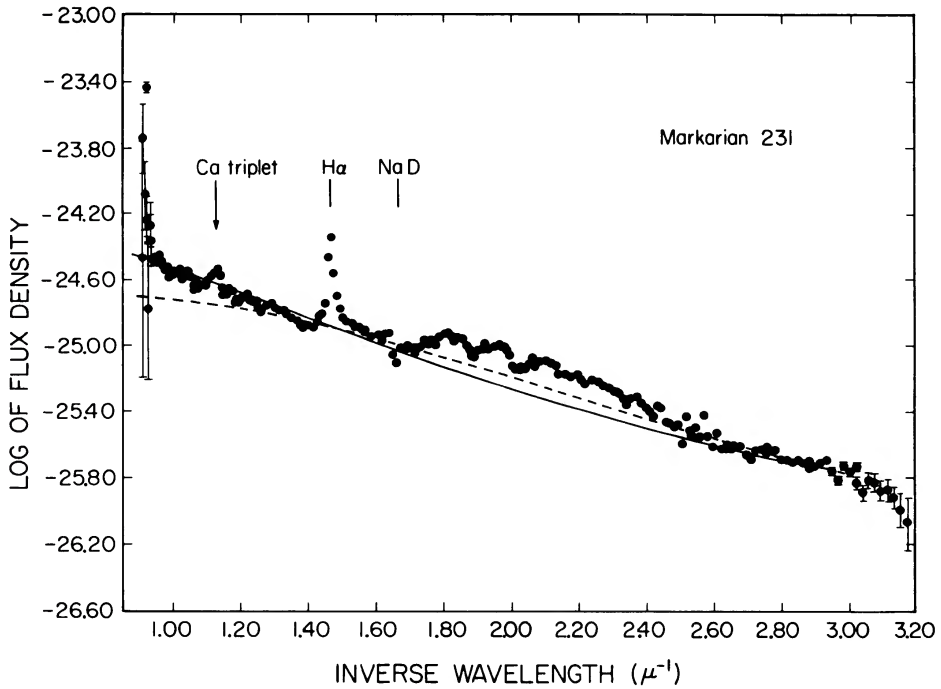

Figure 2. A scan of Markarian 231 obtained with the Multichannel Spectrophotometer (MCSP). The bands are 20 Å in the blue and 40 Å in the red. Prominent spectral features are identified – note in particular the infrared calcium triplet in emission. Continua representing a 10 000 K blackbody reddened by $A_V = 2.1$ (dashed line) and an f_ν = constant spectrum reddened by $A_V = 2.3$ (solid line) are shown.

5 Å (210 Å/mm) and 0.4 Å (16 Å/mm). Full details of the dispersions used and the wavelengths covered by each spectrum are given in Table 1. The IPCS, the observational procedures, methods of wavelength calibration and sky subtraction have already been described elsewhere (Boksenberg 1972; Boksenberg & Burgess 1973; Boksenberg *et al.* 1975a). The observing apertures for the spectra were 1 arcsec dec by 3 arcsec RA and the sky aperture lay 58 arcsec away in RA. Fig. 3 shows one of the low-dispersion spectra and identifies the strongest features in the range 3300–6900 Å. It has been normalized to absolute units using the scans described above. Figs 4 and 5 show normalized higher dispersion spectra of wavelength regions covering the strong absorption lines: λ 3889, *H* and *K* in Fig. 4 and the *D*-lines in Fig. 5. Both are from data taken with a dispersion of 50 Å/mm.

3 The continuum

The MCSP data confirm that the continuum of Markarian 231 is remarkably red for a Seyfert galaxy as found by Weedman (1973). However, the continuum cannot be explained

Table 1. Details of spectra of Markarian 231.

Date (1975)	Dispersion (Å/mm)	Wavelength range (Å)
February 9/10	210	3200–7100
April 2/3	50	3500–4550
April 3/4	150	4600–7200
April 4/5	50	5450–6350
April 4/5	210	3300–7200
April 5/6	16	3930–4230
April 5/6	50	4300–5300
April 6/7	50	4900–5850
June 10/11	150	5250–8100

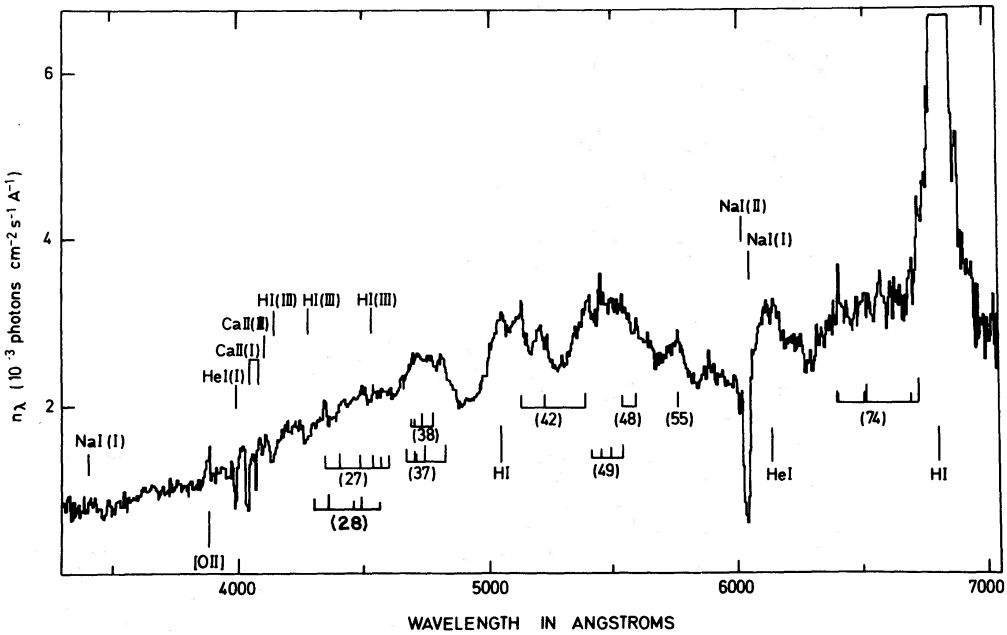

Figure 3. The spectrum of the nucleus of Markarian 231 taken at an original dispersion of 210 Å/mm (~ 5 Å per channel) with the Image Photon Counting System (IPCS). It is normalized to energy units (νf_ν) using the scan of Fig. 2. Strong emission and absorption features are identified – the numbered multiplets refer to permitted transitions in Fe II. Bracketed roman numerals indicate the absorption system to which the line belongs.

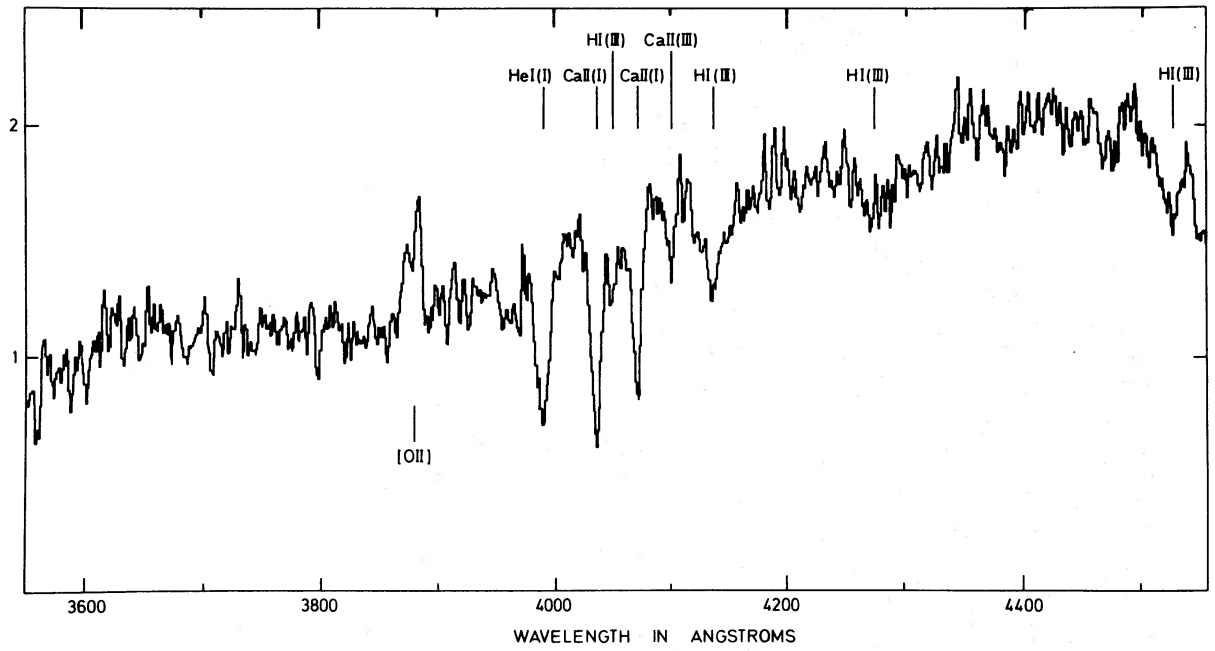

Figure 4. The normalized IPCS spectrum of the nucleus of Markarian 231 showing various absorption lines, in particular He I λ 3889 and Ca II *H* and *K*, and the double structure in the λ 3727 [O II] emission. The optical dispersion was 50 Å/mm and the lines are identified as in Fig. 3.

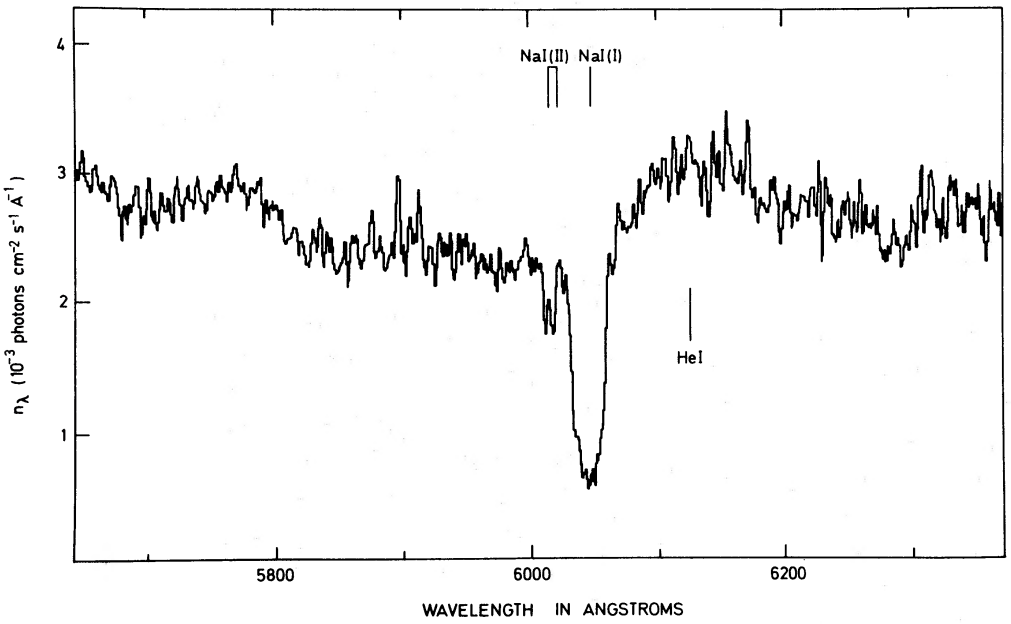

Figure 5. The normalized IPCS spectrum of the nucleus of Markarian 231 showing the absorption line of Na I *D*. The original dispersion was 50 Å/mm and the lines are identified as in Fig. 3.

by a population of late-type stars as in an elliptical galaxy. The overall shape of the energy distribution is quite different from that of such a galaxy alone, in particular the slope of the continuum of Markarian 231 between 6000 and 10 000 Å is much greater than that of an elliptical (Oke & Sandage 1968). Moreover there is no sign in the data of absorption features like Mg I b and the *G*-band normally seen strongly in spectra of such galaxies.

A fit to the continua near the two ends of the spectral range covered in the MCSP data shows that, if a power law spectrum is appropriate, the observed flux $f_\nu \propto \nu^{-2.5}$. There is

considerable evidence for high absorption in Markarian 231 however – both the silicate absorption and the optical absorption lines – and the spectrum can equally well be fitted by a f_ν = *constant* spectrum suffering absorption from a normal galactic absorption law with $A_V = 2.3$. This interpretation has the advantage of bringing Markarian 231 into line with other Fe II emission objects like 3C 273 and I Zw 0051+12 which have flat continua (Wampler & Oke 1967; Oke 1972; Sargent, unpublished).

Both the reddened and unreddened power law continua, whilst fitting the infrared and ultraviolet scan points well, run low in the region between 4000 and 6000 Å. Even in the 'windows' between emission lines at wavelengths 4750 and 5100 Å in the rest system the power laws are 20–30 per cent too low. An alternative model for the continuum involving reddened hot stars, specifically a 10 000 K blackbody reddened by $A_V \sim 2.1$, fits the blue-green region better but runs low at the infrared end of the spectrum near 1 μm. Because it is natural to expect additional sources of radiation at long wavelengths from cooler stars, free–free emission or the source of the long-wavelength infrared flux, hot stars may be preferred as the source of the optical radiation we see from the nucleus of Markarian 231. The two possible fits to the continuum are illustrated in Fig. 2. The alternative of a power-law (non-thermal) source is not yet ruled out however: tests based on variability or polarization may be able to distinguish the two possibilities.

Both models demand quite high absorptions which would inctease the intrinsic luminosity that should be ascribed to Markarian 231. Even without allowing for reddening the absolute visual magnitude of the Seyfert galaxy is $M_V = -23.0$: if $A_V = 2.1$ then $M_V = -25.1$ and Markarian 231 would have the optical luminosity of many quasars (Sandage 1972); Rieke & Low (1976) note a similar high infrared luminosity. The nature of the continuum in and the luminosity of the galaxy will be discussed further in Sections 4 and 6.

4 Emission lines

Since the emission lines in Markarian 231 are broad and badly blended, it is impracticable to measure their intensities individually or to identify weak features. An attractive approach is to synthesize the spectrum, varying a few parameters until a satisfactory fit to the observed spectrum is produced. The obvious ions present in emission are H I, He I, Fe II and [O II], and these were used for the synthesis. All are common features in other extragalactic objects (Boksenberg *et al.* 1975a). The Balmer series and He I are each characterized by one parameter for intensity and one for width, and a case B decrement is assumed for both (e.g. Osterbrock 1974). These were fitted to Hα, Hβ and λ 5876. The widths used, in km/s, were 4200 for H I and 6200 for He I, these being the full widths at half maximum (FWHM) of the Gaussian profiles adopted. A width of 3300 km/s for the Fe II lines seemed appropriate, but this figure could be as high as for the Balmer emission. In particular the lines of multiplet 42 seem broader than this figure. A different intensity parameter was required for each upper term of the Fe II lines used. The important upper terms were z^6P^0, z^6D^0, z^6F^0, z^4D^0 and z^4F^0. The ratios of individual lines originating from each upper term were determined from four sources: the *Revised Multiplet Table* (Moore 1959), the compilation of emission-line strengths by Meinel, Aveni & Stockton (1969), the data of Warner (1967) and observations of the stars HD 37974, CD -52° 9243 and HDE 316285 made with an image-dissector scanner on the Anglo-Australian telescope. Not all the intensities are reliably determined. Nonetheless a satisfactory fit can be obtained throughout most of the spectrum. The best fit is shown in Fig. 6 in which the synthesis is superposed on Fig. 3. The derived line intensities are listed in Table 2.

Several implications of the synthesis deserve mention.

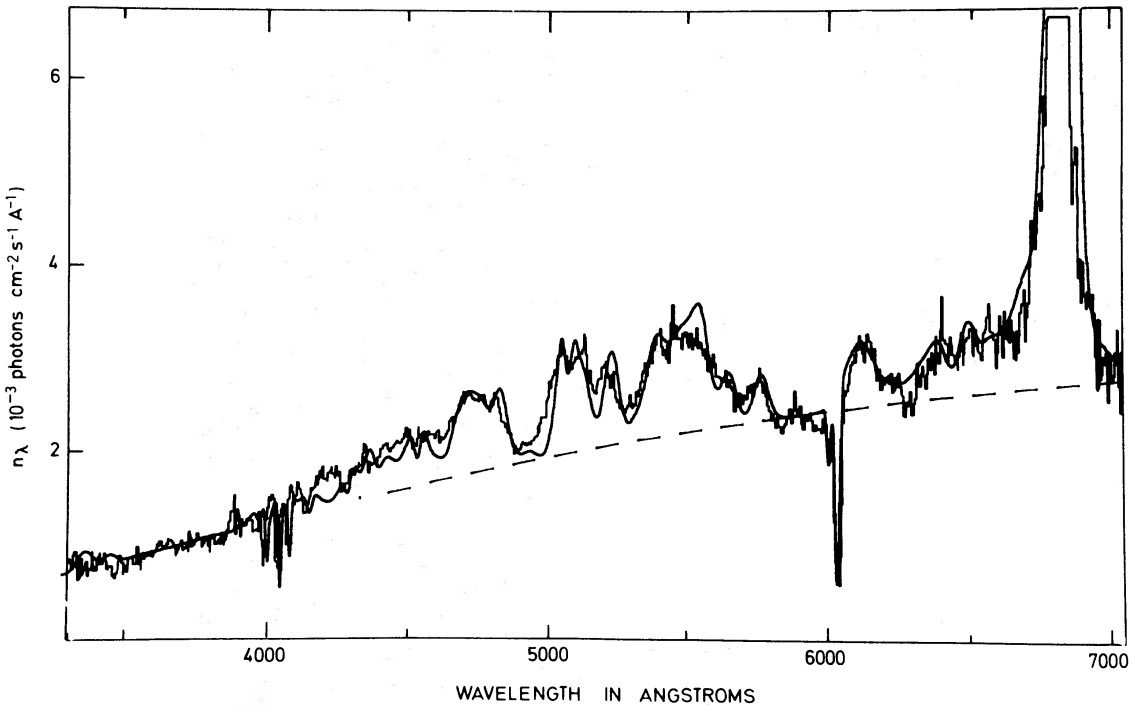

Figure 6. A synthetic spectrum generated as detailed in the text using the line intensities of Table 2 superimposed on the data of Fig. 3.

4.1 THE CHOICE OF CONTINUUM

An underlying continuum was selected; the emission lines were added to it and a reddening law finally applied to make it match the data. The selection of the continuum flux distribution and the corresponding reddening determine the relative line intensities. If the observed continuum, $f_\nu \propto \nu^{-2.5}$, is adopted, the fit is poor, the red lines being too weak and the blue lines too strong. A good fit is found by adopting either $f_\nu = constant$ or a 10 000 K blackbody for the underlying continuum. Both continua are very similar over most of the observed range. Thus the emission lines appear to be reddened along with the continuum.

4.2 BALMER LINES

Adams (1972) reported absorptions at Hγ to H13 at velocities somewhat in excess of the emission redshift. These are also seen in our data and are discussed in the next section. The Hβ/Fe II λ 4924 blend can be matched only if there is also strong absorption in Hβ at 300 ± 100 km/s higher redshift than the emission. The two peaks which might otherwise be thought to be these lines are generated by an absorption superposed on a much stronger and rather broader emission feature; they are not the two lines themselves and cannot be used for radial velocity determinations. For a normal radiative Balmer decrement, Hβ should be almost twice the height of the observed feature in the absence of absorption. If this absorption were produced by material intervening between the emission region and the observer, as in a classical shell spectrum, its effect on Hα would be much more marked than is observed. Instead, it must act on the underlying continuum only. The geometry of a galaxy in which absorbing material lies between the continuum source and the emission regions seems contrived. Balmer absorption is probably an intrinsic property of the continuum source itself so that this supports the notion that early-type stars emit the continuum we observe. For the synthesis, Balmer line absorption of FWHM 2300 km/s redshifted by 300 km/s relative to the

Table 2. Line and multiplet intensities in Markarian 231.

Species	Multiplet	Wavelength of strongest line (Å)	Observed intensity (Hβ = 100)	Flux (10^{-14} erg cm^{-2} s^{-1})	Notes
H I	Hα	6563	615	210	(1), (2), (3)
	Hβ	4861	100	34	(3)
	Hγ	4340	33	11	(3)
	Hδ	4101	16	5	(3)
He I	2^3P^0–3^3D	5876	50	17	
	2^3P^0–4^3D	4471	10	3	
	2^3S–3^3P^0	3889	16	5	
[O II]	1F	3727	3	1	
Ca II	2	8542	129	44	(1)
Fe II	1	3277	9	3	
	6	3193/4	21	7	
	14	3783	4	1.4	
	25	5001	3	1	
	26	4461	4	1.4	
	27	4233	40	14	
	28	4179	56	19	
	29	3825	6	2	
	35	5133	13	4	
	37	4629	103	35	
	38	4584	33	11	
	40	6516	47	11	
	42	5018	96	33	
	43	4731	7	2	
	46	6084	32	11	
	48	5317	26	9	
	49	5276	154	53	
	55	5535	20	7	
	74	6456	69	24	
	153	3814	3:	1:	
	154	3748	1:	0.5:	
	unclassified	5101	8	3	
	unclassified	6318	18	6	
	unclassified	6384	6	2	
Ni II	4	3407	14	5	

Notes to Table 2:

(1) Not deduced from synthesis – measured directly from MCSP data.
(2) Used to calibrate the Hβ = 100 intensity scale in terms of cgs units.
(3) Corrected for the absorption lines centred 300 km/s to the red of the emission line.

emission lines was applied to the continuum prior to the addition of the emission lines. The adopted profiles of the line absorption coefficients of Hβ–H10 were Gaussian and had central optical depths 0.6, 0.3, 0.22, 0.19, 0.16, 0.14 and 0.12 respectively. The figure for Hα could not be determined from the observations independent of the emission intensity the others were fitted to the spectrum. A small contribution to Hε from Ca II absorption may be present.

4.3 OTHER EMISSION LINES

Multiplet 4 of Ni II seems to be present in the IPCS data. The two strongest lines are λλ 3407 and 3769, and these might also explain unidentified features in 3C 273: the '3760 Å' feature described by Boksenberg *et al.* (1975a) – tentatively identified therein as Ti II – and the 'λ 3405' feature found by Baldwin (1975a). More important are deficiencies in the fit around 4230–4300 Å and 4400–4430 Å. These can most easily be explained by the strongest lines of [Fe II], of similar width to the Fe II and therefore probably occurring in the same region. No suitable analysis exists for Fe II, but the weakness of [Fe II] suggests an electron density, n_e, in the range 10^6–$10^7\,\mathrm{cm}^{-3}$.

The major respect in which the synthesis differs from the original data is that the latter is low in the spectral range 3700–3900 Å. This could represent either absorption by the higher members of the Balmer series or the presence of emission in the Balmer continuum. The first suggestion is of interest in view of the Balmer line absorption which has been included explicitly for only the lower members of the series; the second relates to the detection of Balmer continuum emission in a number of low-redshift quasars by Baldwin (1975b).

The intensity of Hβ found in the synthesis leads to an emission measure $\int n_e^2\,dV$ of $2.2\times10^{67}\,\mathrm{cm}^{-3}$ (if the Hubble constant is 50 km/(sMpc)). If the emitting gas has $n_e\sim10^7\,\mathrm{cm}^{-3}$, this indicates a mass of gas of $\sim2000\,M_\odot$ in a volume equal to that of a sphere with radius 0.1 pc. The radius of the emission line region will of course be greater than this if the filling factor is less than 1. Outside the spectral range covered by the IPCS data, one unequivocal feature in the MCSP data can be identified with the infrared calcium triplet ($3d^2D$–$4p^2P^0$). One major puzzle however is the lack of *H* and *K* emission which comes from the same upper state as the triplet emission and should, according to the branching ratio, be 100 times stronger. This problem is already known to arise in galactic objects (e.g. Herbig 1975). It can be understood only if the nebula is very optically thick in *H* and *K*, in particular $\tau_H\gtrsim100$. It would be possible to deduce the density from the Ca II lines if the forbidden lines λ 7291 and 7323 ($4s^2S$–$3d^2D$) could be measured. Unhappily as a result of the redshift these lines lie underneath the atmospheric A-band and no useful limit on their strength can be obtained.

The forbidden doublet λ 3727 of [O II] seen in Markarian 231 is a low-density feature which, taken together with the absence of the red [O II] doublets, indicates $n_e<10^4\,\mathrm{cm}^{-3}$. Adams (1972) reports this emission line to be spatially extended; plainly it arises in a different region of the galaxy from that emitting the other lines. In fact λ 3727 is also narrower than the other emission lines and on the 50 Å/mm IPCS data in Fig. 3 it is clearly seen to be double at redshifts of 11 900 and 12 700 km/s. One interpretation would be that gas in Markarian 231 fairly far from the nucleus is being driven away from the centre of the galaxy at velocities of 400 km/s as a result of the violent activity there. This notion could be tested if the velocity field from the [O II] emission in the other parts of the galaxy were to be mapped.

5 Absorption lines

The four strongest absorption lines in Markarian 231 form an absorption system, which will be termed here 'System I', at a redshift ~8000 km/s. The highest resolution spectrum obtained with the IPCS covers three strong absorptions of Ca II *H* and *K* and He I λ 3889 in System I. They are shown in Fig. 7 replotted on a velocity scale. It is clear at once that these are of a different nature from those seen in most high-redshift quasars (e.g. Boksenberg & Sargent 1975). In those objects the absorption lines arise only from ground or excited fine structure states and are usually very narrow, many being less than 50 km/s broad. Also strong lines usually go to zero intensity at their centres. By contrast in Markarian 231 all

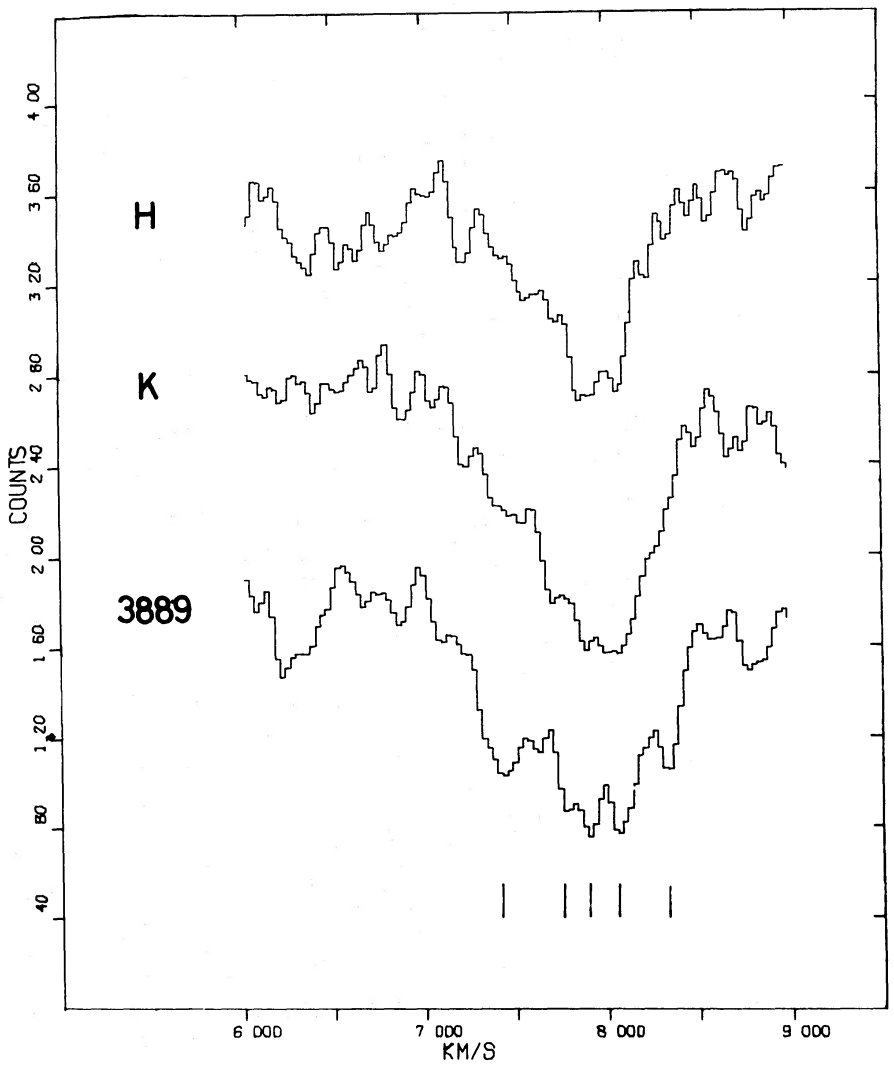

Figure 7. The profiles of the *H*, *K* and λ 3889 lines plotted on the same velocity scale with the *K* and *H* lines displaced upwards by 100 and 200 counts respectively. Positions of the possible velocity components mentioned in the text are marked. These data were originally taken at a dispersion of 16 Å/mm.

four of the strong absorption lines are broad (~ 1500 km/s) and none is deeper than 60 per cent of the observed continuum at their darkest part. In addition the He I line arises from a metastable level 23 eV above the ground state. These lines more resemble those seen in NGC 4151 by Kraft & Anderson (1969) which are ~ 600 km/s broad and include λ 3889. There is some evidence in the λ 3889, *H* and *K* absorptions for structure with 'components' at redshifts of 7420, 7760, 7900, 8060 and 8320 km/s.

If any similar component structure is present in the System I *D*-line absorption it is confused by the doublet nature of the transition with a separation which corresponds to 300 km/s. Our data do however show that the weak absorption to the blue of the main *D*-line absorption found by Adams (1972) is double with a separation which is appropriate if it is identified with D_1 and D_2 at a redshift of 6250 km/s. This we shall call 'System II'. Possible absorption due to He I λ 3889 may be present in this system (fig. 7) but none is detected due to Ca II. The cloud producing the System II absorption has a velocity ~ 6500 km/s towards the Earth with respect to the emission redshift. The lines are resolved and about 150 km/s wide.

Balmer line absorption at a velocity of 200 km/s in excess of the emission line redshift has already been discussed; it will hereafter be referred to as System III. There are absorptions at Hγ, Hβ and Hε visible in Figs 2 and 3. Adams (1972) claimed to see H8 and H10 to H13 also: the present data suggest the presence of H8 and H10 and the fact that the synthesis discussed in Section 4 falls higher than the data just longward of the Balmer limit also supports Adams' claims. Figs 2 and 3 also show that the *K*-line of Ca II is present in absorption in System III. The Hε absorption is blended with the CA II *H*-line. It is possible that the feature Adams identified with H8 contains a contribution from λ3889 of He I but there is no evidence for other helium absorptions. Table 3 gives the redshift deduced from the strongest members of the system: the mean value is 12 900 ± 160 km/s, indicating an emission line redshift of 12 600 ± 200 km/s. The synthesis (Section 4) shows the System III absorptions to be broad. It is not possible from our data however to distinguish between a relatively sharp Gaussian profile and the broad wing profile which would be present if the System III absorptions were stellar.

Table 3. The System III absorption redshift.

Line	Observed wavelength (Å)	Redshift (km/s)
λ4340 Hγ	4532	13 270
λ4101 Hδ	4280	13 090
λ3969 Hε + H	4139	12 850
λ3933 K	4102	12 890
λ3889 H8 + He I	4050	12 420
Mean		12 900
Standard error of mean		±160

In Section 4, arguments were advanced that the System III lines arose in the hot stars that emit the observed continuum. The equivalent widths are indeed compatible with luminosity class III—V A stars, and their widths must be the result of the velocity dispersion of the stars. The observed luminosity of $10^{12} L_\odot$ indicates a total mass of A stars emitting the continuum $\sim 10^{11} M_\odot$. The velocity dispersion deduced from the synthesis then implies a length scale ~ 200 pc, corresponding to 0″.2 on the sky which would not be resolved. On the other hand Balmer line absorption is seen in NGC 4151 (Kraft & Anderson 1969) presumably against the non-thermal source so that the System III lines could also originate in an intervening cloud in a similar way. As commented above, however, such a cloud would have to absorb the continuum source alone and not the emission-line region.

The presence of absorption from a high-lying metastable level in System I and possibly also in System II argues strongly in favour of closely associating the absorbing clouds with the nuclear activity in Markarian 231. The two systems then represent material approaching us at velocities ~ 4800 and ~ 6500 km/s with respect to the mean emission-line region. The fact that He^+, Ca^+ and Na^0 coexist within individual absorbing clouds suggests that the gas is being illuminated by a dilute radiation field with a rather high colour temperature. It is interesting to draw the analogy here with the λ3889 absorptions seen (Wilson *et al.* 1959) in the Orion Nebula Trapezium stars and the He I, Ca II and Na I absorptions sometimes seen in the shell spectra of shell-stars (Underhill 1966). The possible origin of this dilute radiation field is discussed in Section 6.

This conclusion taken together with the presence of calcium triplet emission probably excited by resonance fluorescence suggests that these absorbing clouds are a geometrically

favoured sample of the broad emission line region. The relative velocities of the clouds would produce the broadening of the emission lines as has been hypothesized by Oke & Sargent (1968), Anderson (1970) and others.

Table 4 lists the equivalent widths of the absorption lines and the flux they extract from the continuum. The equivalent widths of Ca II *H* and *K* in System I can be used to infer the optical depth in these features along the line of sight by the doublet ratio method (Strömgren 1948). Putting the values of equivalent widths from Table 4 into Strömgren's Table 2 shows that the doublet ratio is 1.7, $\tau_H \sim 0.6$ and the radial velocity dispersion parameters of the absorbers (the Doppler width) is 330 km/s generally similar to the observed line widths of *H* and *K*. Thus in spite of the result from the emission lines that in the emission region the optical depth is very large, along the line of sight viewed from the Earth it is much less.

A similar analysis using the ratio of the Na I *D*-lines to the λ 3302/3 blend for System I shows that the *D*-lines are much more optically thick. The *D* to λ 3302/3 ratio is 15.0, $\tau_D = 37$ and the Doppler width is 210 km/s: the last in quite good agreement with the result from the calcium lines. In view of the high value of τ_D found, it is interesting that the *D*-line is not black in its centre. Either the absorbing cloud does not cover the source or some other source of light (e.g. λ 5876 emission or starlight) from a more extended region is present.

The deduced column densities of Ca II and Na I are 8×10^{13} and $1.3 \times 10^{15}\,\mathrm{cm}^{-2}$ respectively. If the gas doing the absorbing has normal abundances and a normal dust-to-gas ratio this indicates a minimum hydrogen column density of $2 \times 10^{21}\,\mathrm{cm}^{-2}$ and a minimum visual absorption of about 2 mag. Thus the column densities tie in well with the results from the continuum deduced in Section 3. If the density in this column is $n_e \sim 10^7\,\mathrm{cm}^{-3}$, the thickness of the cloud is of order 10^{14} cm.

Table 4. Strengths of absorption lines.

System	Line		Equivalent width (Å)	Flux extracted from continuum (10^{-14} erg cm^{-2} s^{-1})
I	λ 7665	K I	<3	<3
	λ 5890/6	Na I	18	16
	λ 4226	Ca I	<0.5	<0.4
	λ 3968	Ca II	3.6	2.3
	λ 3933	Ca II	6.1	3.8
	λ 3889	He I	6.3	3.8
	λ 3302/3	Na I	1.2:	0.5:
II	λ 5896	Na I	0.7	0.6
	λ 5890	Na I	0.8	0.7
	λ 3889	He I	0.3:	0.2:
III*	λ 6563	H I	(60)	
	λ 4861	H I	35.	
	λ 4340	H I	15.	
	λ 4101	H I	6.	
	λ 3970	H I	5.	
	λ 3968	Ca II		
	λ 3933	Ca II	1.	
	λ 3889	H I	4.:	
	λ 3889	He I		
	λ 3835	H I	4.:	
	λ 3798	H I	4.:	

Note:

* System III equivalent widths *with respect to the true continuum only* from the synthesis.

The D_1 and D_2 lines in System II are essentially equal indicating a high optical depth in this cloud also. The Na I column density in this cloud must exceed about $2 \times 10^{13}\,\mathrm{cm}^{-2}$.

A column density from the System III lines is meaningless if they are formed in hot stars but on the intervening cloud model the equivalent width of K indicates a Ca II column density in excess of $10^{13}\,\mathrm{cm}^{-2}$.

6 Discussion

6.1. FLUORESCENCE

The simultaneous presence of calcium triplet emission and resonance line (H and K) absorption suggests that fluorescence plays an important part in producing the line emission. Even if collisions contribute to the triplet emission, this in no way affects the arguments for high optical depth. Detailed inspection of Tables 2 and 4 shows that about a factor 7 more energy is emitted in the infrared triplet than appears to be absorbed in the resonance lines. The absorption, however, could be higher in other directions than the one sampled from Earth or the calcium ions could be absorbing a different or less absorbed continuum source.

These suggestions tie in with other deductions already made about conditions in Markarian 231. For example the difference between the values of τ_H deduced from emission and absorption lines already suggests that the continuous emission observed is viewed through a smaller column than is present in the emission line region. However, if in most other directions the H and K lines absorbed all the continuum radiation over a range of velocities of 4000 km/s (the difference between System I and the emission redshift), still only about half the required number of photons can be extracted from the observed continuum to power the triplet emission. Moreover, if it is thought that the Fe II (in particular the multiplet 42) emission is also caused by fluorescence (Wampler & Oke 1967) then a similar calculation shows that with any reasonable extrapolation of the observed spectrum to the ultraviolet there is insufficient flux there to produce multiplet 42 lines at the observed strength even if the exciting line λ 2343 is completely absorbed for 4000 km/s.

Because of the evidence however (Section 4) that the continuum observed at Earth is reddened by the same amount as the lines, the energy absorbed in the resonance lines may be increased if the fluorescence takes place in the unreddened radiation field. Then there are adequate photons present to explain both the calcium fluorescence, if the optical depth in the resonance lines is only modestly greater in other directions, and the multiplet 42 fluorescence with a somewhat thicker λ 2343 line.

Alternatively there could be a further source of radiation seen by the gas which is so absorbed as to be invisible from Earth. Although there is no direct evidence for such a source, one would note that other objects with strong Fe II emission have clearly non-thermal continua. If it were accepted that the observed continuum came from stars, then it would be tempting to suppose that a non-thermal source exists in Markarian 231 which provides the ultraviolet radiation required to excite the emission lines, but which is completely obscured in our direction so that if viewed at a different angle it would more closely resemble, say, 3C 273 or I Zw 0051+12.

Possibly all these reasons play some part in explaining the imbalance between energy absorbed and emitted. It is interesting to note that other Fe II emission objects (which also show calcium triplet emission (Sargent, unpublished)) do not have strong H and K absorption lines thus suggesting an imbalance in the fluorescence process in the same sense as Markarian 231.

6.2 GEOMETRY

The evidence for very high column densities of material in Markarian 231 from the calcium triplet emission and silicate absorption seems quite conclusive. The silicate absorption particularly suggests that much of the sky at the nucleus is covered with clouds with $A_V \gtrsim 10$ magnitudes. However, the continuum source seen from Earth is viewed through a relatively modest obscuration.

If the hot-star model for the continuum is accepted then one is led towards the type of model shown in Fig. 8(a). This includes the unobserved non-thermal source inferred from the appearance of other objects in Section 6.1.

For the model in which the observed continuum comes from the non-thermal source the two different values of the absorption can be reconciled if we see through a hole or down a tunnel to the nucleus. The choice between these two depends on how organized is the overall nebula surrounding the nucleus. For example the nebula could be a thick disk which has as its axis of symmetry pointing nearly towards Earth—Fig. 8(b)—or there could be a jumble of independent clouds with a few random directions covered less well than most.

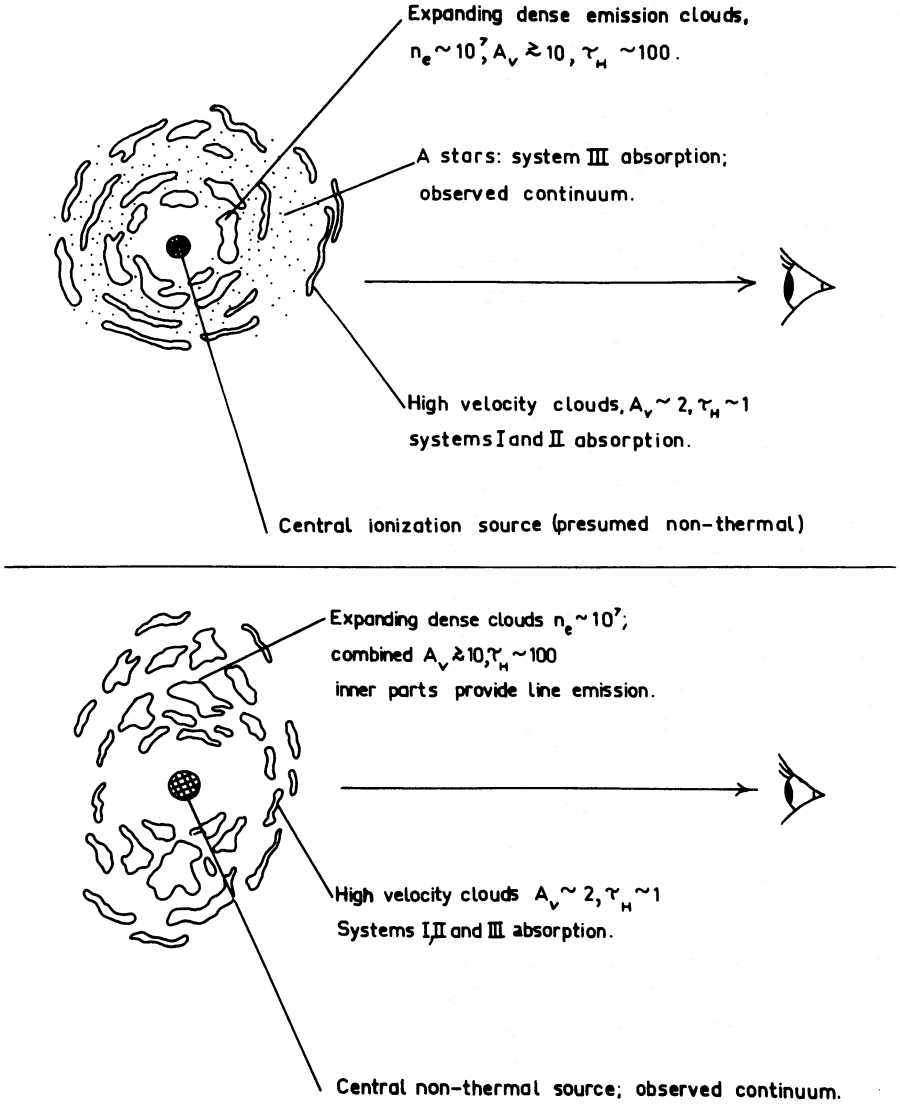

Figure 8. (a) A possible geometrical layout of the nuclear region of Markarian 231 in which the source of the observed continuum is taken to be hot stars. (b) As (a) if the observed continuum comes from a non-thermal source.

In either case, as argued in Section 5, the clouds which produce the System I and II absorptions form an outer part of the emission-line region and represent a thinner portion of it through which A_v is only ~ 2 mag.

6.3. IMPLICATIONS FOR OTHER OBJECTS

Boksenberg *et al.* (1975b) suggested that the relative prominence in different Seyfert galaxies of the broad permitted lines and the narrow forbidden lines is related to the proportion of sky seen from the central source that is covered by the dense material of the broad line region. Markarian 231 is extreme in the sense that no sharp forbidden line emission except for [O II] is seen. The O^+ may not be produced as a result of the ultraviolet radiation from the nucleus at all, so that in Markarian 231 *all* the Lyman continuum photons may be absorbed in the dense inner region.

In fact most other Fe II galaxies do show weak [O III] lines (Boksenberg *et al.* 1975a; Allen & Fosbury, unpublished). This indicates larger holes in the dense region which ties in with the evidence that they are observed essentially unobscured (i.e. flat spectra, no absorption lines). Nonetheless the calcium triplet emission in these objects (Sargent, unpublished) indicates that high-optical-depth regions exist there too. Thus objects like 3C 273 and I Zw 0051+12 might show some of the characteristics of Markarian 231 if viewed from other directions.

Can more extreme objects than Markarian 231 be found? If the ultraviolet continuum and emission lines in Markarian 231 were much more absorbed, no evidence for nuclear activity might be found in the optical region at all! The infrared emission however could not be hidden. Possibly objects like M82, NGC 253 and Cen A are low-luminosity examples of such cases. In addition some Class 2 Seyferts like NGC 1068 might represent cases where the nuclear regions are completely hidden as viewed from Earth, although the ultraviolet flux might leak out to other directions to excite the emission line spectrum.

The high luminosity of Markarian 231 puts it in the quasar class. It is tempting to suggest it is a quasar and that other close-by examples are also hiding from us behind absorbing clouds in their parent galaxies.

7 Future work

The data presented in this paper, particularly that relating to the absorption lines, could be improved by spectra with higher signal-to-noise. The possibility that other absorption systems could be present at the *D*-lines could be answered by longer integration at about 50 Å/mm. Additionally the blue region from λ 3302/3 to H_γ could be better observed – a more accurate equivalent width for λ 3302/3 would be useful, System II absorptions at *H* and *K* should be searched for and the profiles of the Balmer line absorptions in System III should be examined. This could be studied at 50 Å/mm or slightly higher resolution.

Searches for variability and polarization of the nucleus are highly desirable in order to distinguish between the two possible models for the optical continuum.

This paper has only touched on a proper analysis of the absorption lines from a physical point of view. The simultaneous presence of *D*-line and λ 3889 absorptions in Systems I and II is not properly understood.

Finally the suggestion that there may be other objects like Markarian 231 but with the nucleus totally obscured at optical wavelengths should be investigated by infrared surveys of galaxies. If there are very bright hidden Seyfert nuclei in otherwise normal galaxies this may be the best way of finding them.

Acknowledgments

We are grateful to our time assignment panels for generous allocations of telescope time. Valuable assistance at the telescope, in the preparation of equipment and the reduction of data was given by Clive Amos, Bob Argyle, Steve Briggs, John Fordham, Godfrey Green, David Lewis, Dennis McMullan, John Pilkington, Keith Shortridge, Martin Ward, Peter Wehinger, Pete Willmoth and Andrew Wilson. A valuable conversation with Gerry Neugebauer is gladly acknowledged. We acknowledge the Wise Observatory and Smithsonian Research Foundation grant SF-0-3005.

References

Adams, T. F., 1972. *Astrophys. J. Lett.*, **176**, L1.
Adams, T. F. & Weedman, D. W., 1972. *Astrophys. J. Lett.*, **173**, L109.
Allen, D. A., 1976. *Astrophys. J.*, **207**, 367.
Anderson, K., 1970. *Astrophys. J.*, **162**, 743.
Baldwin, J. A., 1975a. *Astrophys. J. Lett.*, **196**, L91.
Baldwin, J. A., 1975b. *Astrophys. J.*, **201**, 26.
Boksenberg, A., 1972. *Proc. ESO/CERN Conf., Auxiliary instrumentation for large telescopes*, Geneva, 1972 May 2–5, p. 295.
Boksenberg, A. & Burgess, D. E., 1973. *Proc. Symp., Astronomical observations with television-type sensors*, Vancouver, 1973 May 15–17, p. 21.
Boksenberg, A. & Sargent, W. L. W., 1975. *Astrophys. J.*, **198**, 31.
Boksenberg, A., Shortridge, K., Fosbury, R. A. E., Penston, M. V. & Savage, A., 1975a. *Mon. Not. R. astr. Soc.*, **173**, 289.
Boksenberg, A., Shortridge, K., Allen, D. A., Fosbury, R. A. E., Penston, M. V. & Savage, A., 1975b. *Mon. Not. R. astr. Soc.*, **173**, 381.
Herbig, G. H., 1975. *Astrophys. J.*, **200**, 1.
Khachikian, E. Ye. & Weedman, D. W., 1973. *Astrofiz.*, **7**, 389.
Kraft, R. P. & Anderson, K. S., 1969. *Astrophys. J.*, **158**, 859.
McMullan, D., Powell, J. R. & Curtis, N. A., 1972. *Adv. Electronics Electron Phys.*, **33A**, 37.
Meinel, A. B., Aveni, A. F. & Stockton, M. W., 1969. *Catalog of emission lines in astrophysical objects*, University of Arizona, Tucson.
Moore, C. E., 1959. *A multiplet table of astrophysical interest*, National Bureau of Standards, Washington.
Oke, J. B., 1969. *Publ. astr. Soc. Pacific*, **81**, 11.
Oke, J. B., 1972. *IAU Symp. 44*, p. 139.
Oke, J. B. & Sandage, A., 1968. *Astrophys. J.*, **154**, 21.
Oke, J. B. & Sargent, W. L. W., 1968. *Astrophys. J.*, **151**, 807.
Oke, J. B. & Schild, R. E., 1970. *Astrophys. J.*, **161**, 1015.
Osterbrock, D. E., 1974. *Astrophysics of gaseous nebulae*, W. H. Freeman and Co., San Francisco.
Rieke, G. H. & Low, F. J., 1972. *Astrophys. J. Lett.*, **176**, L95.
Rieke, G. H. & Low, F. J., 1976. *Astrophys. J. Lett.*, **200**, L67.
Sandage, A., 1972. *Astrophys. J.*, **178**, 25.
Sargent, W. L. W., 1968. *Astrophys. J. Lett.*, **152**, L31.
Sargent, W. L. W., 1970. *Astrophys. J.*, **160**, 405.
Strömgren, B., 1948. *Astrophys. J.*, **108**, 242.
Underhill, A. B., 1966. *The early type stars*, p. 234, D. Reidel, Dordrecht, Holland.
Wampler, E. J. & Oke, J. B., 1967. *Astrophys. J.*, **148**, 695.
Warner, B., 1967. *Mon. Not. R. astr. Soc.*, **138**, 229.
Weedman, D. W., 1973. *Astrophys. J.*, **183**, 29.
Wilson, O. C., Munch, G., Flather, E. M. & Coffen, M. F., 1959. *Astrophys. J. Suppl.*, **4**, 199.